New Developments in Experimental and Analytical Aspects of Light Figure Spectroscopy

Nazim Mamedov

Institute of Physics
Azerbaijan National Academy of Sciences

State of Art

- Acquisition and analyses of light figures (LF) have been known as a sensitive method for optical characterization of anisotropic materials for a long time, with the first reports dating back to 19 century. LFs are mentioned by Born and Wolf in well-known "Principles of Optics". To an introductory level , LF techniques and useful applications are well-described in "Optical Crystallography" by Wahlstrom.
- LF characterization of the various materials and structures has been performed, to date. But, this characterization has been done for the most part using only single wavelength or a set of peaked-up wavelengths, without scanning on wavelength. Overwhelmingly, gyration-free materials have been studied. Materials with gyration have practically been left without proper experimental efforts and analytical analyses.
- Four years ago, when we were looking for a suitable experimental method for characterization of the novel structurally two-dimensional thallium-contained ternary compounds with record-breaking memory effects and thermo-power, the situation I was describing forced us to explore the possibilities of extended applications of LFs.

Introduced Innovations

- First was a new LF-based method for determination of the group-to-phase velocity ratio, or the relative dispersion of the refractive indices (***Jpn. J. Appl. Phys.40 (2001) 4938***). At an early stage the method was applied to various representatives of the novel Tl-contained semiconductors-ferroelectrics with unknown optical parameters. The obtained results were good. But, the comprehensive and final approval was received by testing the well-known uniaxial calcite, $CaCO_3$ (***J. Appl. Phys. 91 (2002) 4110***).
- Next was the break-though that came with development of the first analytical approach to LF of materials with gyration. In the work that firstly treated influence of gyration, supposedly high sensitivity of the method was also put to the test. The expectations were confirmed to a cutting-edge value of $\sim 10^{-6}$ in experiments on paratelluride, TeO_2, for which, owing to high sensitivity, transversal component of gyration was determined for the first time (***Jpn. J. Appl. Phys. 42 (2003) 5145***).
- On a par with this and the advanced experimental reinforcement, a series of useful approximations for quick estimates on LF was introduced into standard LF method and approbated on various materials (***J. Cryst. Growth 237-239 (2002) 2023, Jpn. J. Appl. Phys. 41 (2002) 7254, J. Phys. Chem. Sol. 64 (2003) 1959***).

Presentation Structure

- First I will describe the analytical approaches we used for gyration-free materials and materials with gyration. For convenience I will restrict myself to the subjects with transversally isotropic dielectric function, which are uniaxial. However, biaxial materials and films can also be treated. An important expression relevant to the biaxial case and reflecting the on-going generalization of the method will be given, also.
- Next I will present an experimental set-up with digital image processing and the experimental results which were obtained using this set-up. In so-doing I will embrace experimental data for various materials, including materials with incommensurate phase transitions. Special accent will be put on the firstly predicted and observed effect of shrinkage of interference curves into zero-size isochromates, and on the numbering of the interference orders. Both are specific for materials with gyration.
- Finally I will briefly address the topic of the application to thin films, including nanosized thin films, and discuss the ways which seem to be most adequate to the problem. With regard to the nanosized thin films with small optical anisotropy, a full LF approach and experiment, which include investigation of the spatial distribution of the polarization field in LF pattern, will be proposed.

Analytical Approach: Gyration-Free Materials (I)
(Innovative!)

$$
\begin{cases}
A = \dfrac{1}{2\varepsilon_3}\left[\varepsilon_3(\varepsilon_1+\varepsilon_2) - C\sin^2\theta\right] \\
B = \dfrac{1}{2\varepsilon_3}\left\{\left[\varepsilon_3(\varepsilon_2-\varepsilon_1) + C\sin^2\theta\right]^2 + 4\varepsilon_3(\varepsilon_1-\varepsilon_2)(\varepsilon_2-\varepsilon_3)\sin^2\theta\sin^2\varphi\right\} \\
C = (\varepsilon_1-\varepsilon_3)\cos^2\varphi + (\varepsilon_2-\varepsilon_3)\sin^2\varphi
\end{cases}
$$

$\varepsilon_1, \varepsilon_2, \varepsilon_3$ – Principle Components of Dielectric Tensor

Refractive Indices

$$n_{1,2} = \sqrt{A \mp \sqrt{B}}$$

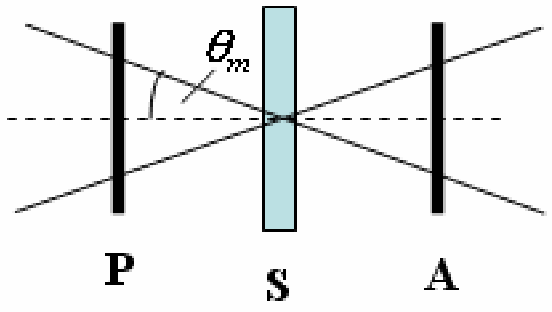

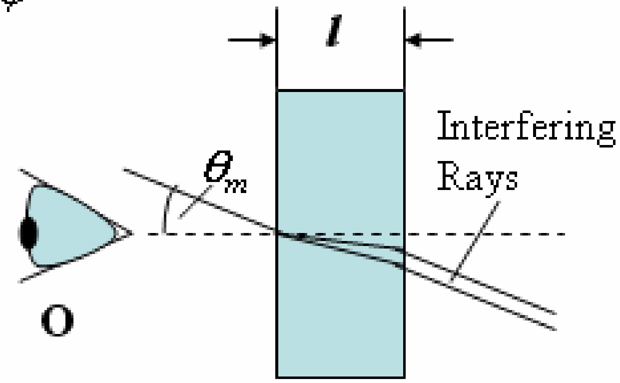

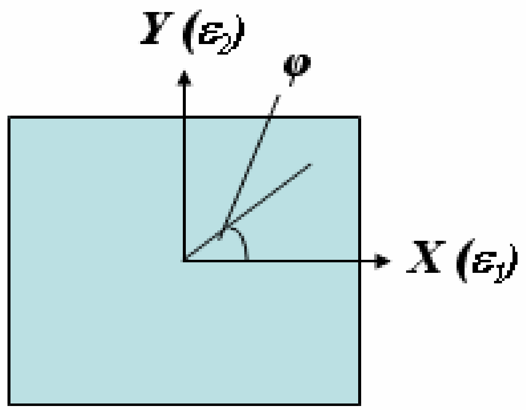

$$
\begin{cases}
n_o = n_{2,1} = \sqrt{\varepsilon_\perp} = \sqrt{\varepsilon} \\
n_e = n_{1,2} = \sqrt{\varepsilon\dfrac{1 \pm \gamma\varepsilon\cos^2\theta}{1 \pm \gamma\varepsilon}}
\end{cases}
$$

Interference Condition

(Uniaxial Case, Optic Axis LF)

$$\left|\sqrt{n_e^2 - \sin^2\theta_m} - \sqrt{n_o^2 - \sin^2\theta_m}\right| = m\frac{\lambda}{l}$$

Wavelength

Interference Order (0,1,2….)

$$\gamma = \left|\frac{\varepsilon_\perp - \varepsilon_{II}}{\varepsilon_\perp \varepsilon_{II}}\right|$$ – Parameter of Anisotropy of Transversally Isotropic Dielectric function

Analytical Approach: Gyration-Free Materials (II)

$$A_m = \frac{n_o^2}{\sqrt{n_o^2 - \sin^2\theta_m}} + \frac{n_e^2}{\sqrt{n_e^2 - \sin^2\theta_m}} \qquad B_m = \left[1 + \frac{\sin^2\theta_m}{4}\left(\frac{1}{\sqrt{n_o^2 - \sin^2\theta_m}} + \frac{1}{\sqrt{n_e^2 - \sin^2\theta_m}}\right)^2\right]^{\frac{1}{2}}$$

Interference Radius

$$R_m = Mr_m = M\frac{l\sin\theta_m}{\sqrt{n_m^2 - \sin^2\theta_m}} + \ldots. \quad \Leftarrow \quad n_m = \frac{A_m}{2B_m}$$

– Mean Path Ray Refractive Index

M – Calibration Constant

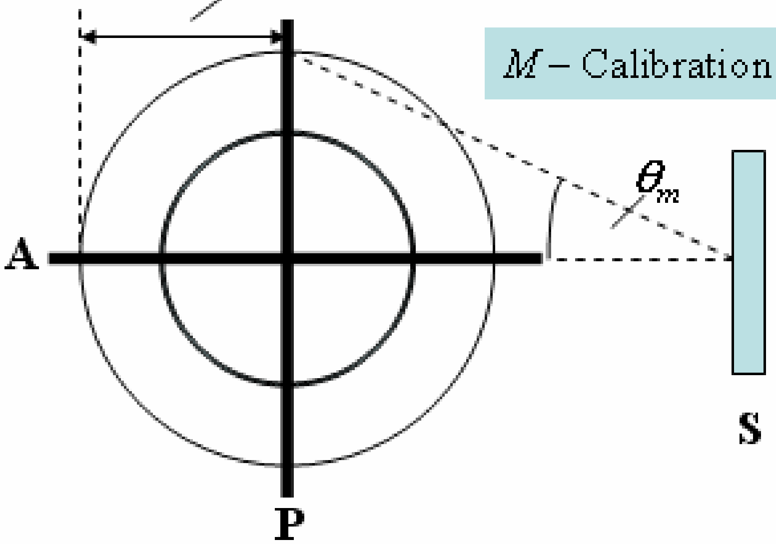

Interference Radius

+

Interference Condition

↓

Full Characterization of Optical Parameters

Analytical Approach: Materials with Gyration (New!)

Interference Radius

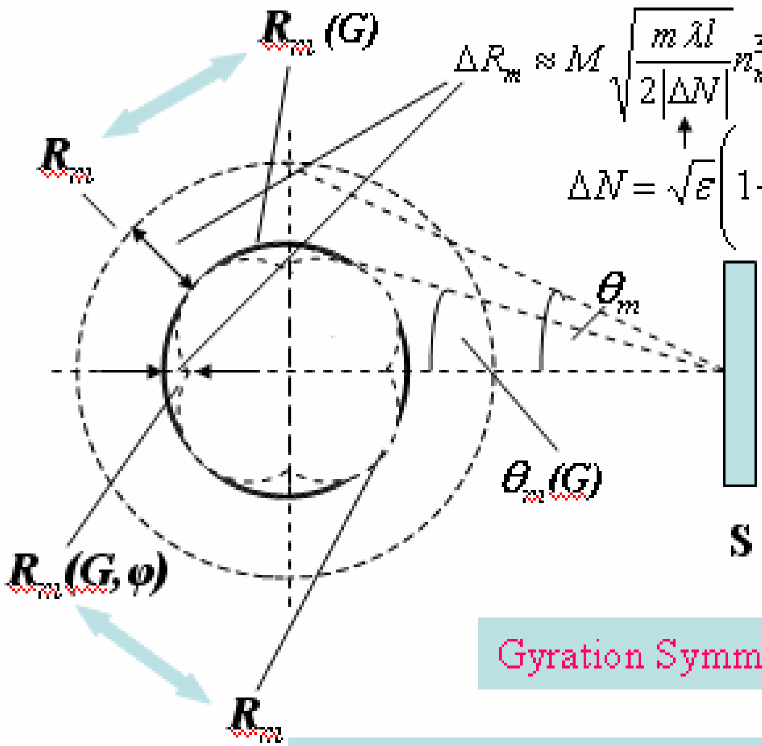

$$\Delta R_m \approx M\sqrt{\frac{m\lambda l}{2|\Delta N|}}\,n_m^3\rho_m G_m$$

$$\Delta N=\sqrt{\varepsilon}\left(1-\frac{1}{\sqrt{1\pm\gamma\varepsilon}}\right)$$

$$n_o=\sqrt{\frac{\varepsilon}{1\mp\varepsilon\rho_o G_o}}\qquad n_e=\sqrt{\varepsilon\frac{1\pm\gamma\varepsilon\cos^2\theta}{(1\pm\gamma\varepsilon)\pm(1\pm\gamma\varepsilon\cos^2\theta)\varepsilon\rho_e G_e}}$$

Corrections for Gyration

Interference Radius | **Interference Condition**

$$\rho_{o,e}=\frac{1}{2G_{o,e}}\left(\sqrt{\gamma^2\sin^2\theta_{o,e}+4G_{o,e}^2}-\gamma\sin^2\theta_{o,e}\right)$$

Gyration Symmetry Independent Ellipticity

Gyration Symmetry Dependent Normal Component of Gyration

$$G_{o,e}=G_{II}+(G_\perp-G_{II})\sin^2\theta_{o,e}\longrightarrow (TeO_2)$$

$$G_{o,e}=G\cos 2\varphi\sin^2\theta_{o,e}\longrightarrow (AgGaS_2)$$

Relative LF Approach
(New!)

Effective Refractive Index

Real Refractive Index

$$N^{eff} = N\left(1-\alpha\frac{\lambda}{N}\frac{dN}{d\lambda}\right)$$

Thickness and Wavelength Dependent Factor

$$\frac{\lambda}{N}\frac{dN}{d\lambda} = -\frac{\lambda}{R_m}\frac{dR_m}{d\lambda} + \lambda\cot\theta_m\frac{d\theta_m}{d\lambda}$$

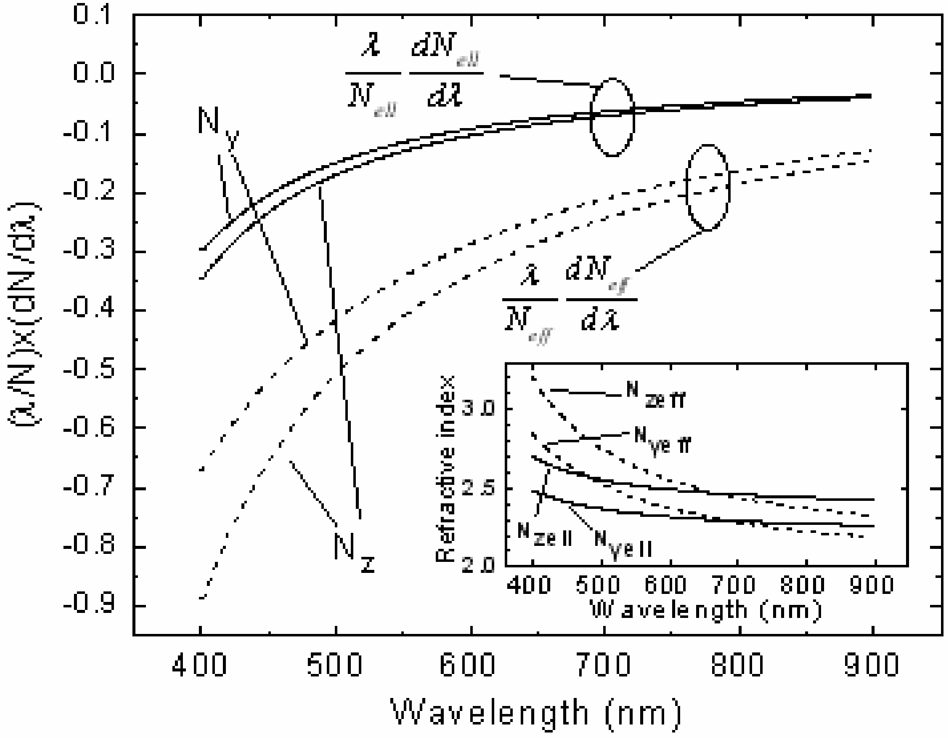

Calibration Constant Independent Relative Dispersion from LF!

Self-consistent experimental determination of refractive indices!

Thin Solid Films 455-456 (2004)244

Better grounds for comparison with theoretically obtained dielectric function and revelation of the particular sources responsible for real dispersion below the energy gap of the materials!

Numerical Approbation on Calcite (I)

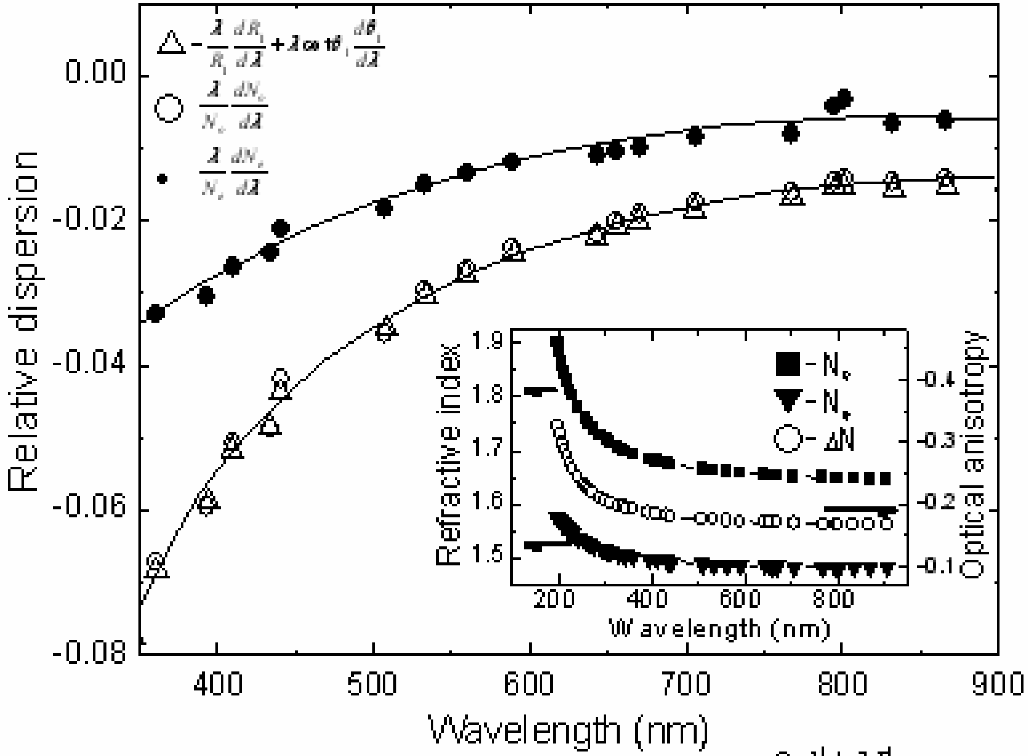

Excellent Agreement for l>60μm!

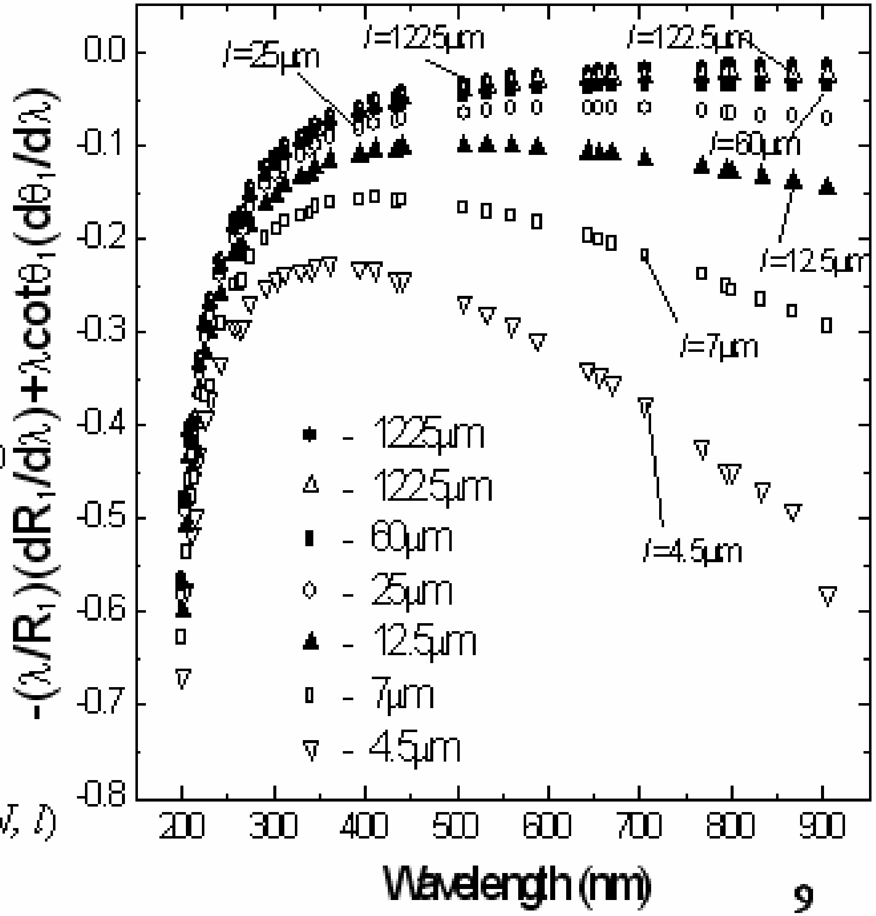

Applicability Condition — $m < \frac{2d|\Delta N|}{\lambda}$

$$\frac{\lambda}{N}\frac{dN}{d\lambda} \rightarrow F(\lambda)$$

$$-\frac{\lambda}{R_m}\frac{dR_m}{d\lambda} + \lambda\cot\theta_m\frac{d\theta_m}{d\lambda} = \frac{\lambda}{N}\frac{dN}{d\lambda}\ \text{(LF)} \rightarrow F(\lambda, N, \Delta N, l)$$

Numerical Approbation on Calcite (II)

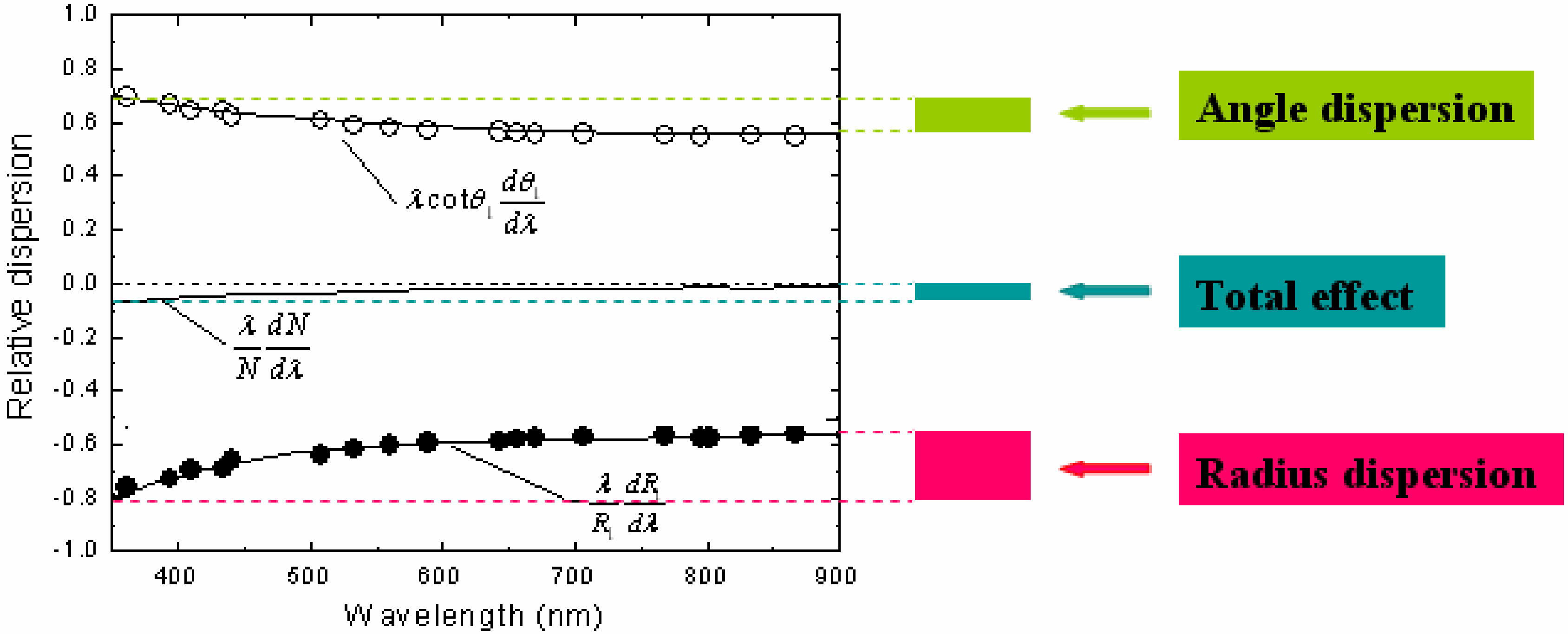

Refractive indices from → Stanley S. Ballard, J.S. Browder, and J.F. Ebersole: American Institute of Physics Handbook, 3rd ed. (McGraw-Hill, New York, 1972) pp. 6-20.

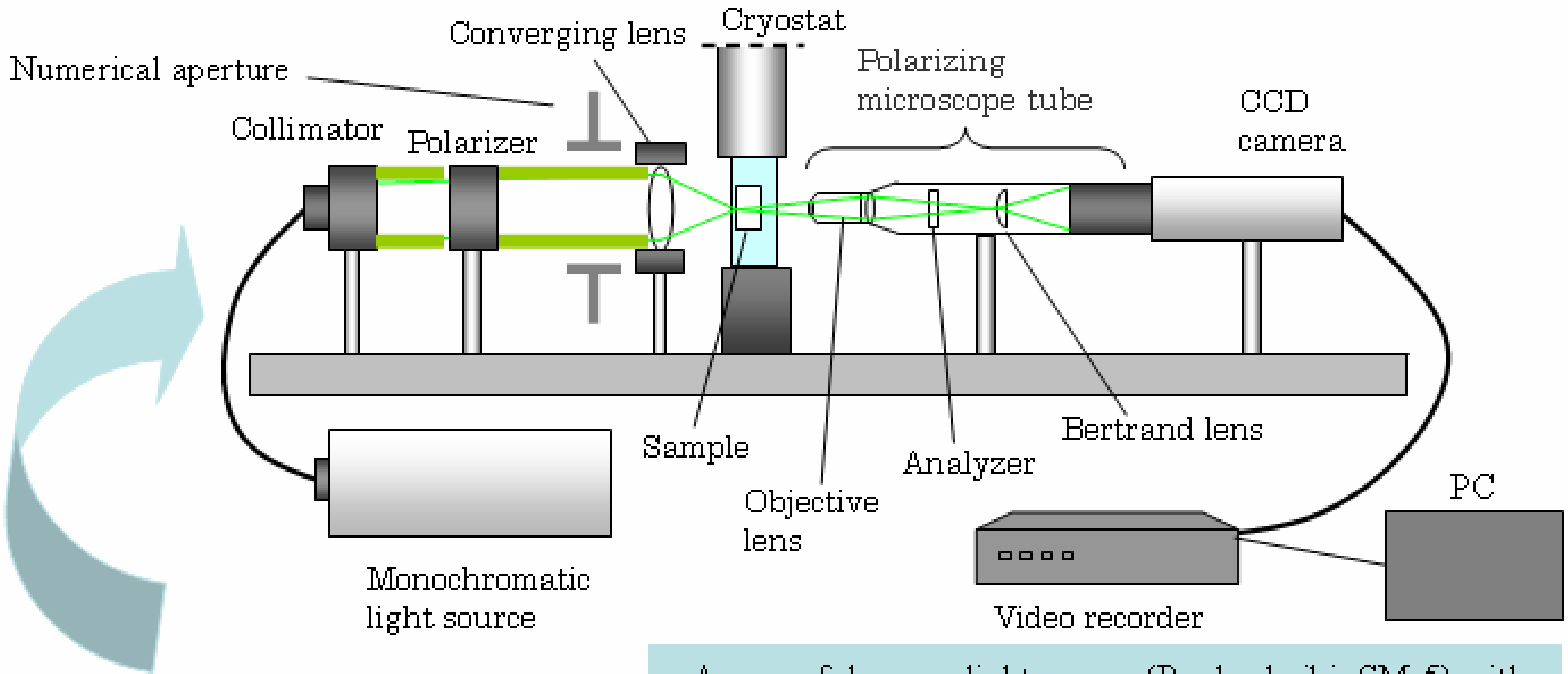

Experimental Set-Up

A powerful xenon light source (Bunko-keiki: SM-5) with built-in monochromator provides all possibilities to obtain high-contrast LF patterns with spectral resolution not more than 4nm in the spectral range 380-850nm.

At the experimental apertures (θ) from 40° to 5° the diffraction limited spatial resolution of the set-up is from ~λ (θ=40°) to~10λ (θ=5°). A special LF-acquisition-compatible cryostat mounted on set-up is designated for temperature-dependent measurements in the range 5-450K. Digital video camera provides on-line monitoring of the LF patterns. Finally, digital treatment using computer (PC) enables us to accurately restore the radial distribution of the light intensity from the recorded LF pattern.

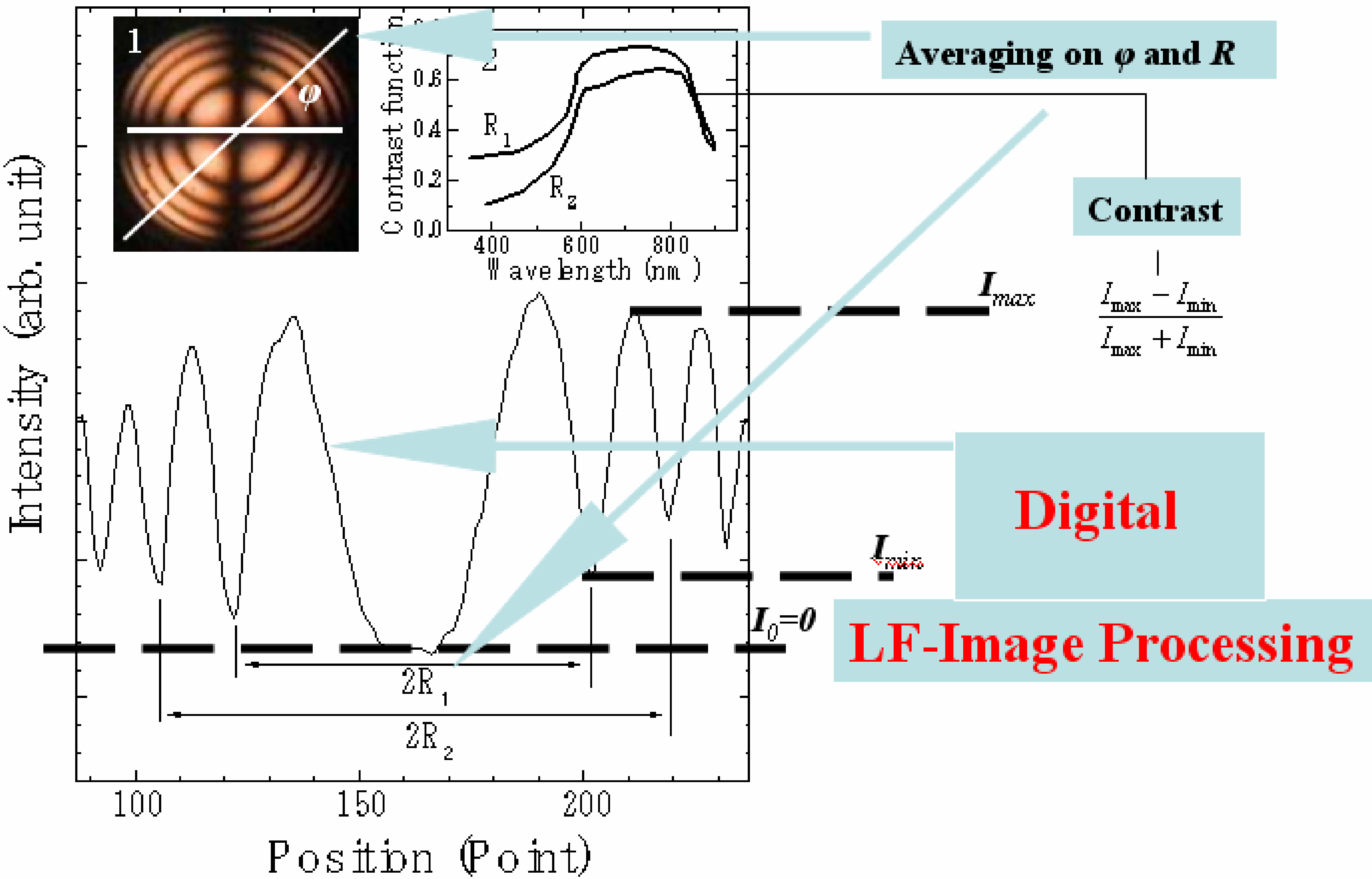
1
φ
Contrast function
0.0
0.2
0.4
0.6
R1
R2
400
600
800
Wavelength (nm)
Averaging on φ and R
Contrast
$\frac{I_{max} - I_{min}}{I_{max} + I_{min}}$
I_{max}
I_{min}
$I_0=0$
Digital
LF-Image Processing
Intensity (arb. unit)
2R1
2R2
100
150
200
Position (Point)

Experimental Approbation of Relative LF Approach

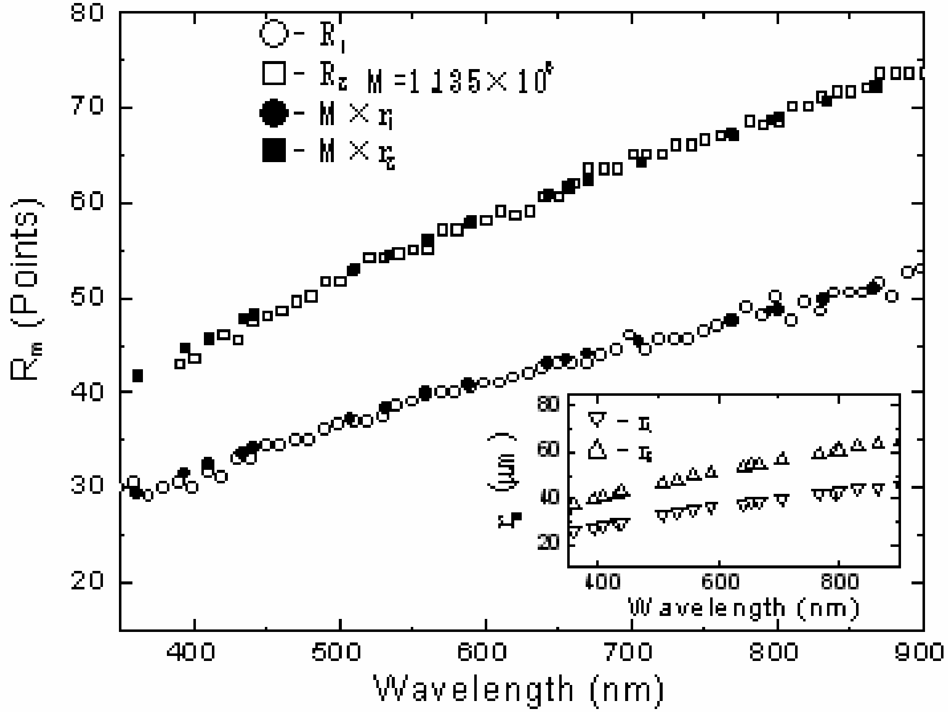

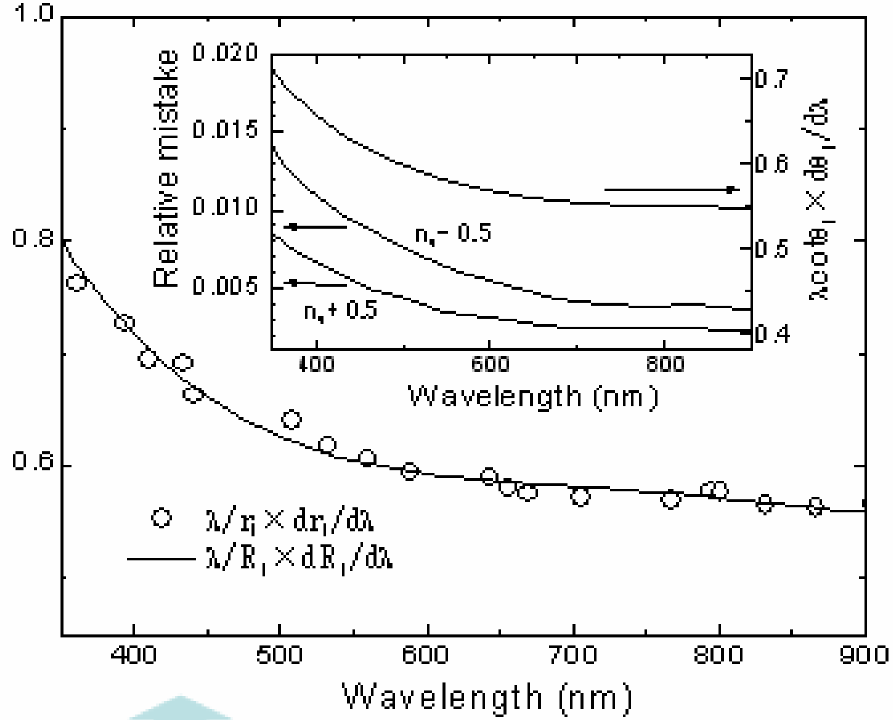

Calculated and Experimental Radiuses are practically the same!

Excellent agreement between calculated and experimental relative dispersion!

First Observation of Shrinkage Effect (I)

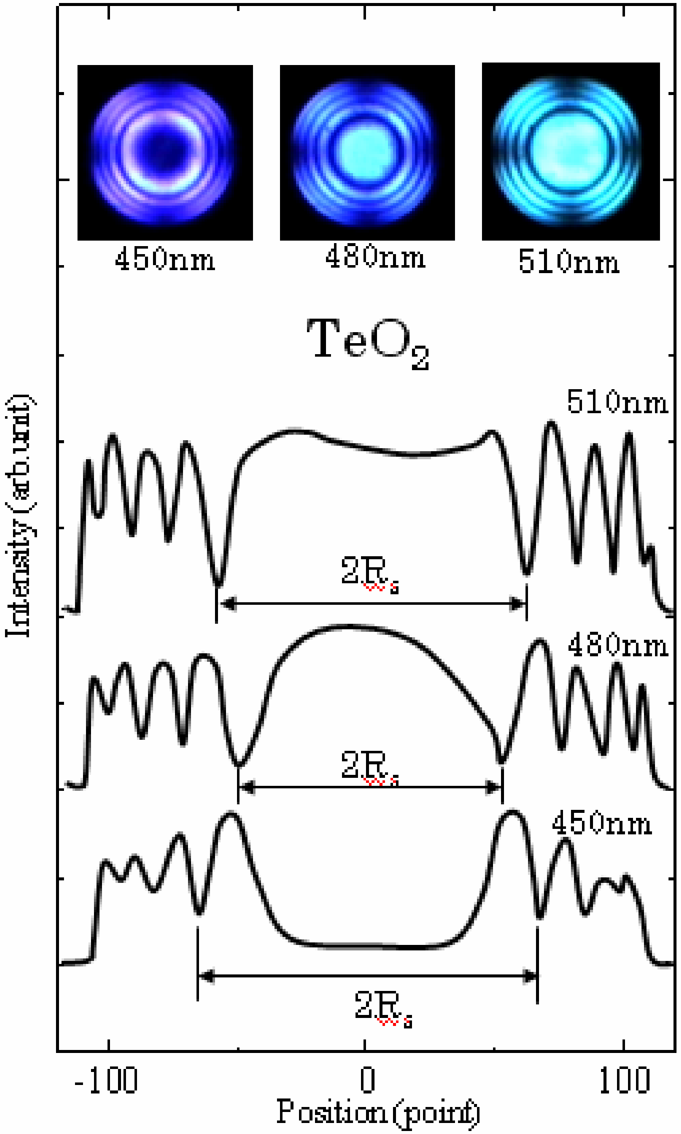

$$l \approx \frac{3 \cdot 10^{-4} m(m+1)}{n_o^3 G_o}$$

Thickness, in mm, for observation of the effect in visible spectral range (400-700nm, $\Delta\lambda$=300nm)

The sample thickness for observation of the effect in the lowest interference order (m=1) is minimal with the value of ~ 0.6 mm for TeO_2 and $AgGaS_2$. The thickness of quarts must be raised to a level of ~15 times the value for TeO_2 or $AgGaS_2$.

Of the last two materials, the best candidate for observation of the effect in optic axis LF is TeO_2. In $AgGaS_2$ the effect might be observed in perpendicular-to-optic axis LF, observation in optic axis LF is practically impossible, as follows from symmetry considerations.

TeO_2 (1.42mm)!

First Observation of Shrinkage Effect (II)

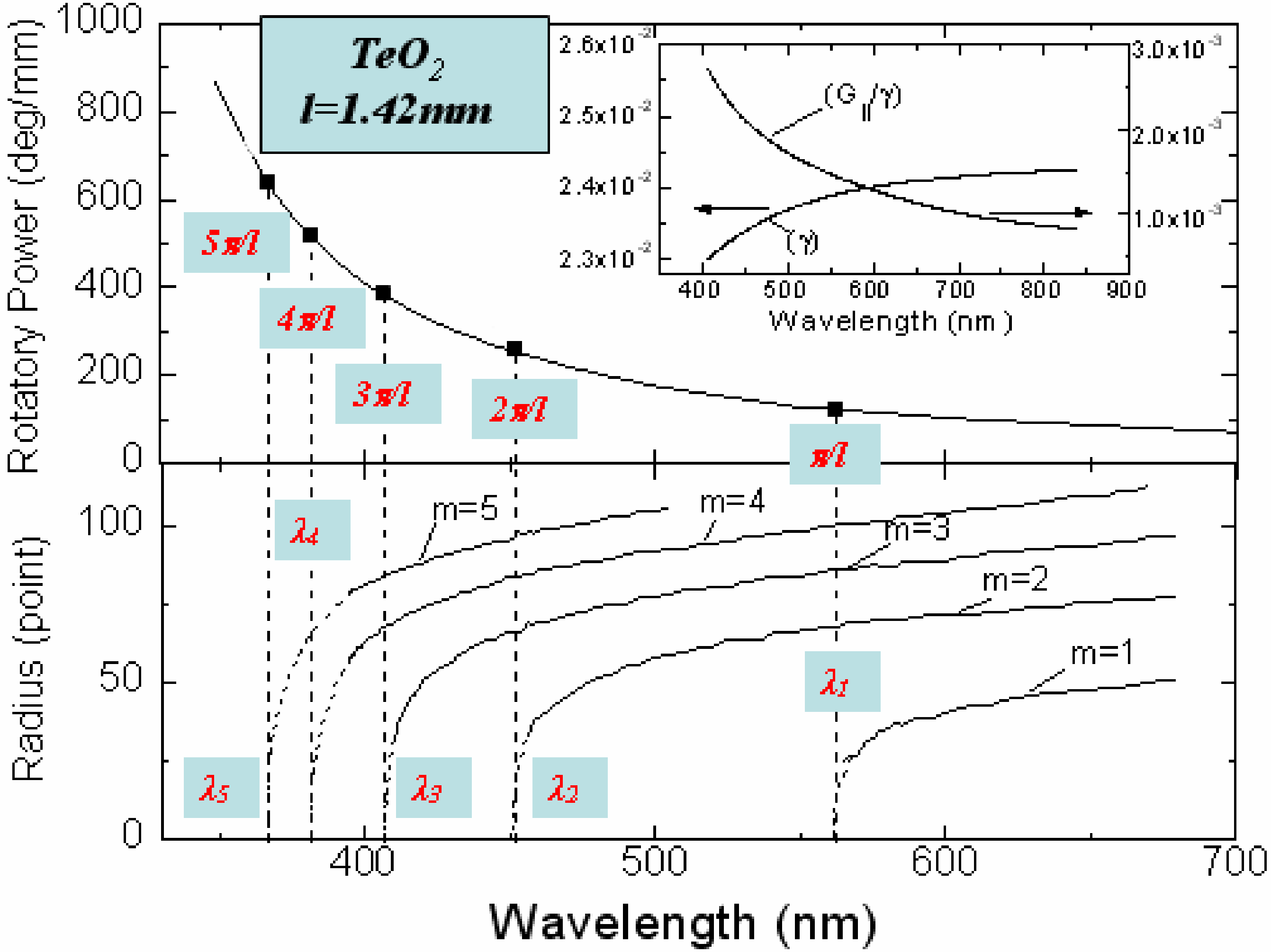

Gyration Effect on LF

$\sim \left|G_{o,e}/\gamma\right|$!!!

Rotatory Power

$$\chi(\lambda_m) = m\frac{\pi}{l}$$

Wavelength Interval

$$\Delta\lambda \sim \frac{1}{m(m+1)}$$

Shrinkage Wavelength

$$\lambda_m \approx \frac{1}{m}\varepsilon^{3/2}(\lambda_m)G_{II}(\lambda_m)l$$

Experimental Determination of Gyration Constants

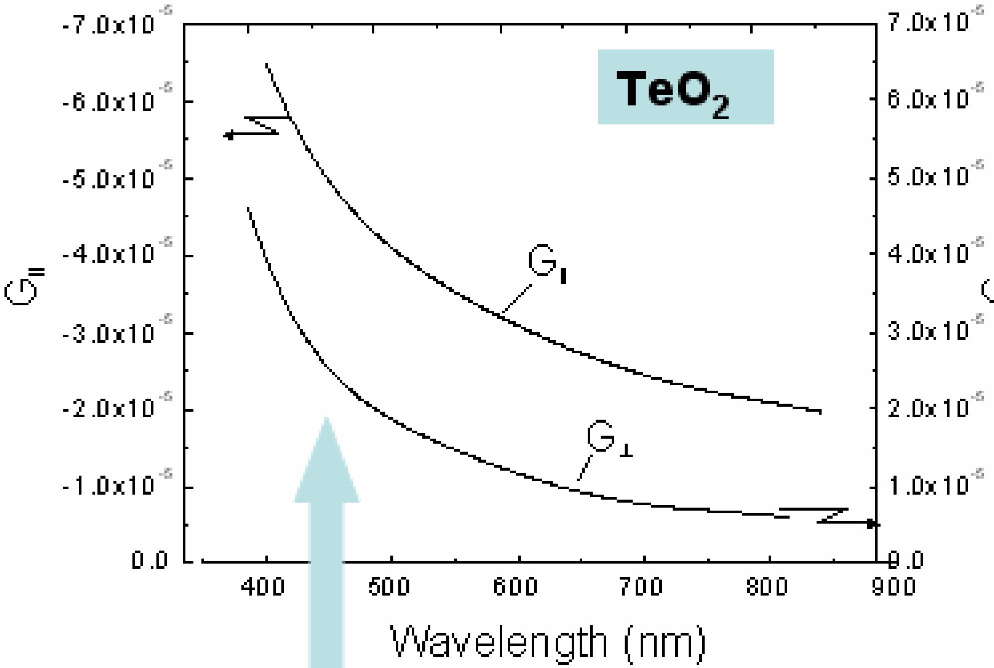

The φ- and θ-dependencies of the normal components $G_{\theta,\varphi}$

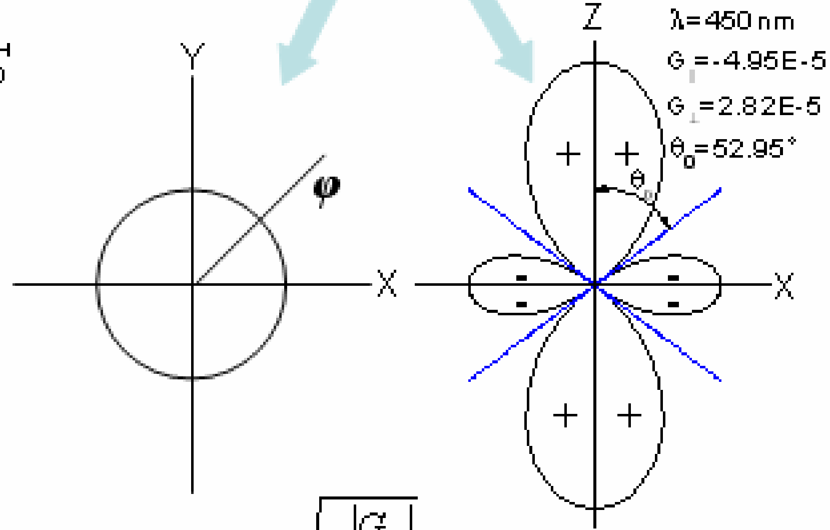

$$\sin\theta_m \approx \sqrt{2\frac{|G_{II}|}{\gamma}}$$

Transversal component obtained from the interference curves sections for which

Experimental Data on Relative Dispersion
(Gyration Case)

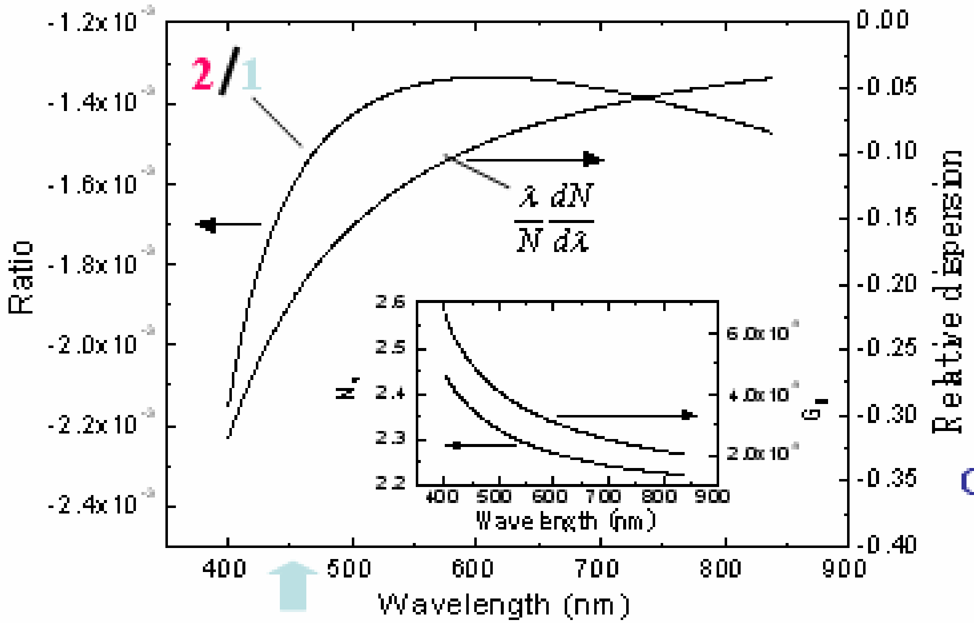

Same as before for gyration-free case!

$$\frac{\lambda}{N_G}\frac{dN_G}{d\lambda} = -\frac{\lambda}{R_m}\frac{dR_m}{d\lambda} + \lambda\cot\theta_m\frac{d\theta_m}{d\lambda}$$

But!

1

$$\frac{\lambda}{N}\frac{dN}{d\lambda} + \frac{N^2\rho G}{1\mp N^2\rho G}\left(\frac{\lambda}{N}\frac{dN}{d\lambda} + \frac{1}{2}\frac{\lambda}{\rho G}\frac{d\rho G}{d\lambda}\right)$$

2

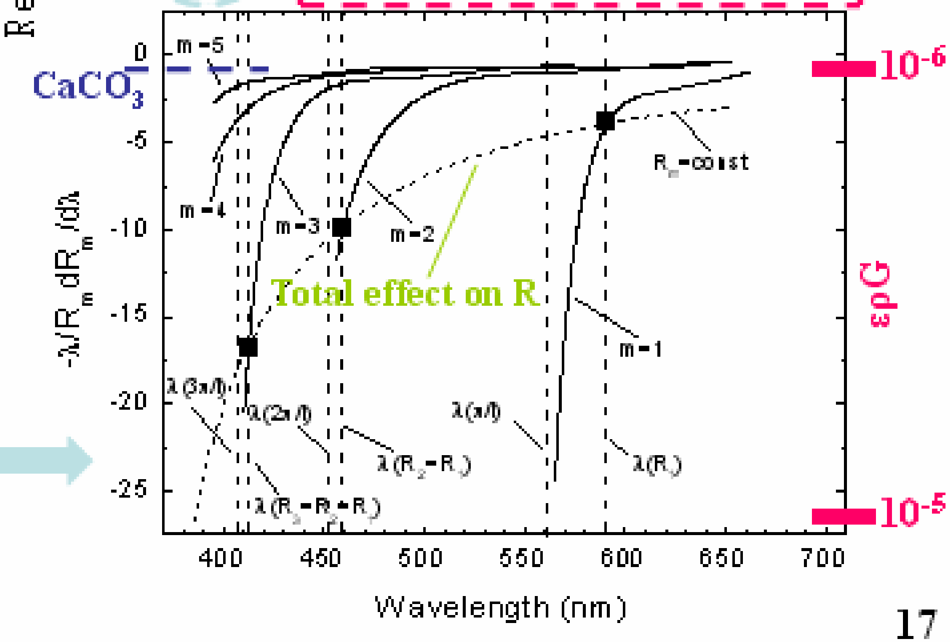

Total effect is negligible!!!

But separately on R_m (or θ_m), the effect is very large and the sensitivity is to a cutting-edge value of 10^{-6}!!!

Numbering of Interference Orders
(New!)

Gyration-free case

$$R_m \approx M \frac{m\lambda}{2\Delta N}\sqrt{1+\sqrt{1+\left(\frac{2l\Delta N}{m\lambda}\right)^2}}$$

$$m << \frac{2d|\Delta N|}{\lambda}$$

$$\sqrt{\frac{m+1}{m}} \le \frac{R_{m+1}}{R_m} \le \frac{m+1}{m}$$

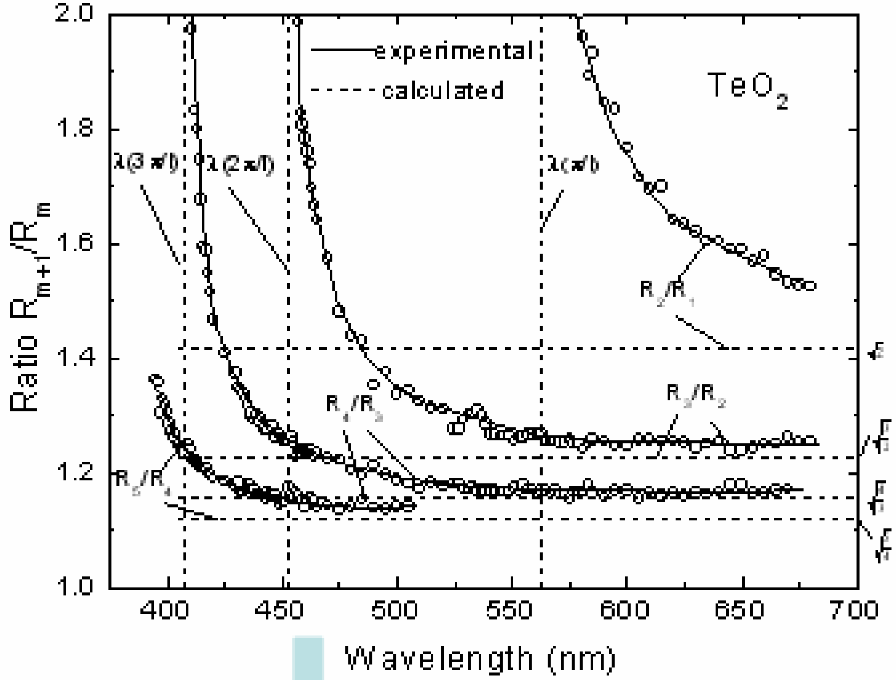

Ratio R_{m+1}/R_m provides reliable basis for correct numbering of interference orders!

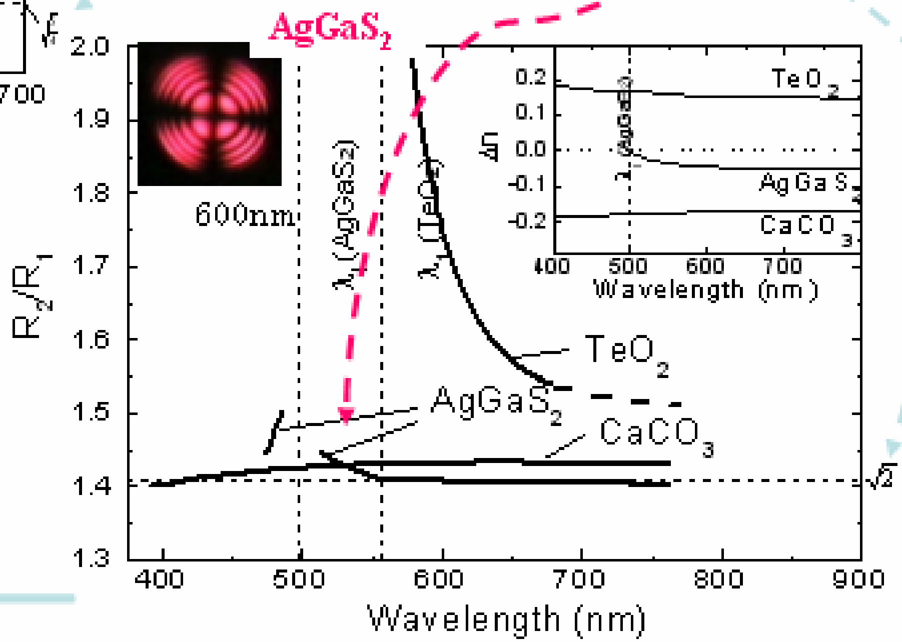

Application to Modulated Structures with Nanosized Correlation Length (I)

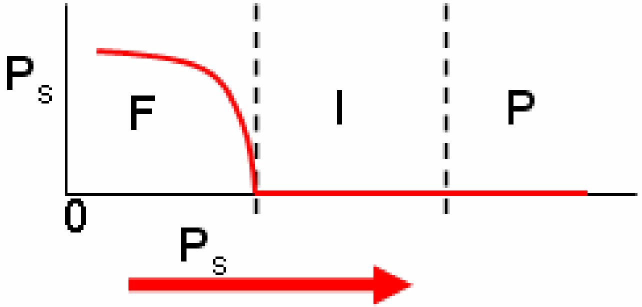

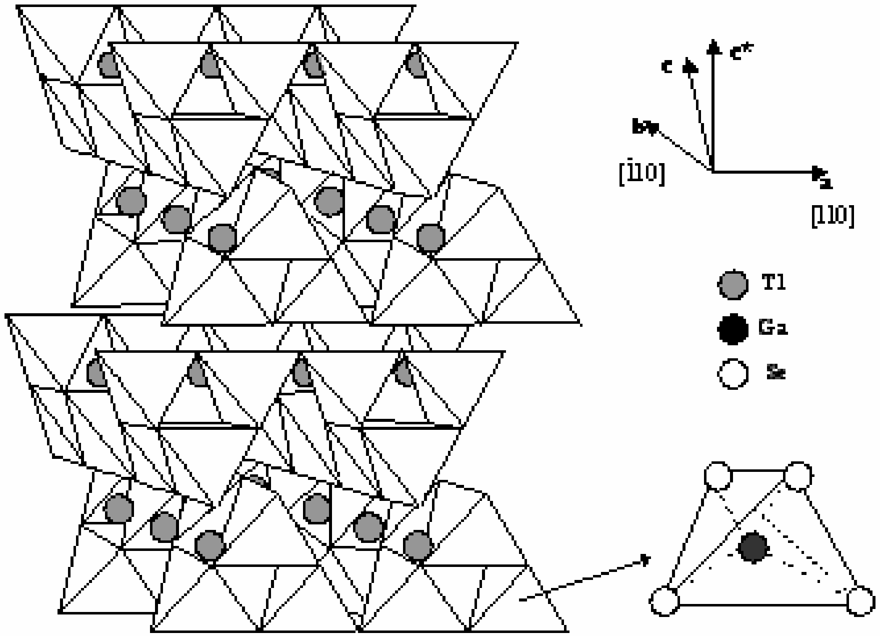

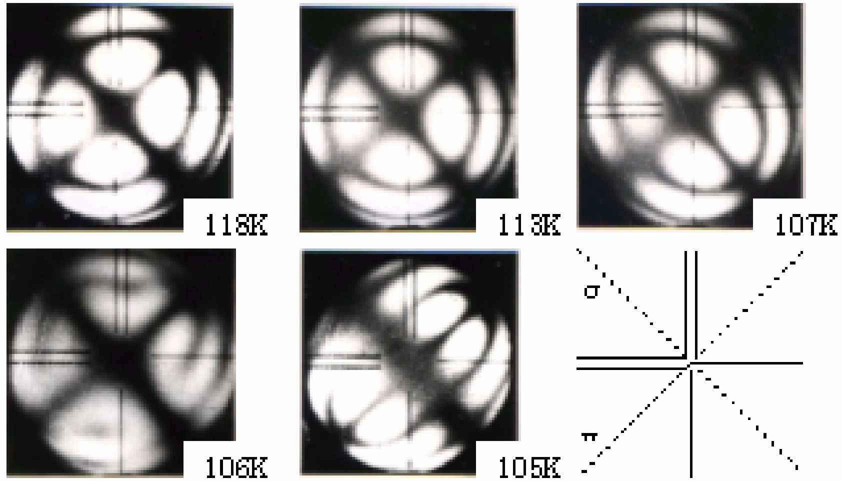

$\Delta N_I \sim 10^{-3}$!!!

I-phase ($TlGaSe_2$): 118-107K

March 23, 2005

Application to Modulated Structures with Nanosized Correlation Length (II)

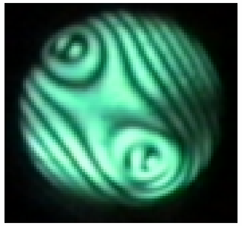

100K

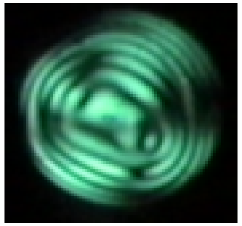

210K

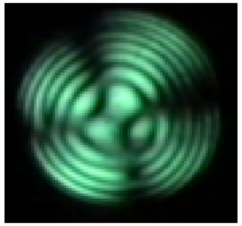

290K

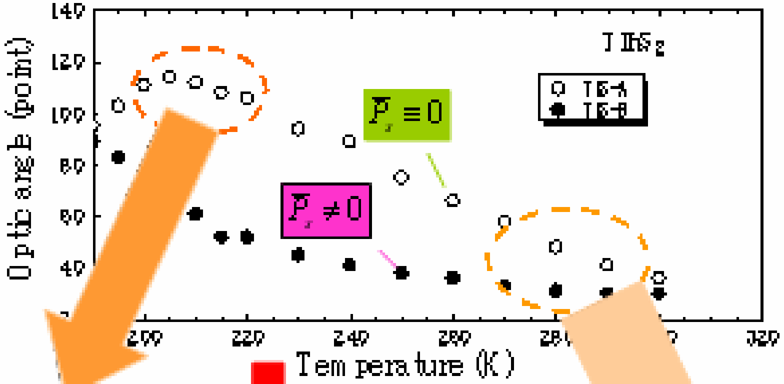

ΔN_I~10^{-3}!!!

I-phase ($TlInS_2$): 200-215K

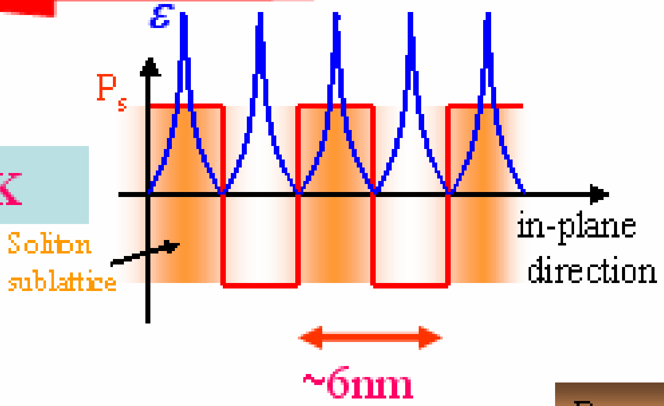

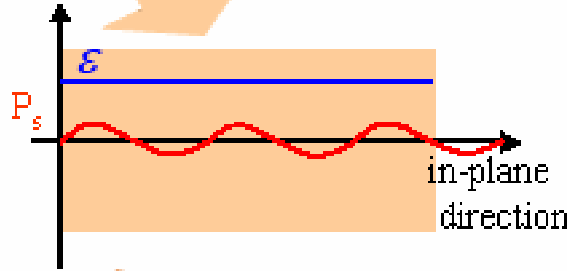

$\bar{P}_s \equiv 0$ → Pure I-phase with soliton sublattice

$\bar{P}_s \neq 0$ → Dirty I-phase without soliton sublattice

Proc. 25[th] Int. Conf. Semiconductor Physics (Springer-Verlag, Heidelberg, 2001) 123

Nanosized spatial dispersion effect (ΔN_I) ~10^{-3} versus ~10^{-6} (V.M. Agranovich, V.L. Ginzburg: Crystal Optics with Spatial Dispersion and Excitons (Springer-Verlag, Tokyo, 1984) **in materials with usual interatomic distances!**

Thin Film Application

Film/Isotropic Substrate

Dry Aperture (n=1) + m=1, λ=0.5μm, γ~0.01, ε~10

Thickness Limit → $l_{film} \geq \frac{2m\lambda}{\gamma\varepsilon\sqrt{\varepsilon}}\frac{1}{n}$ ↔ ~3.3 μm

Film/Anisotropic Substrate – No Thickness Limitation!

Standard LF

(compensatorless, linearly polarized incident beam)

$\sim \ M l_{film} \tan\theta_m \left|1/N_o^{film} - 1/N_e^{film}\right|$

Especially favorable are thin substrates (large interference angles θ_m) for which spatial resolution is of the order of λ and $\tan\theta_m$ is large. But, if, for some reasons, the separation is not observed, then

Extended LF

(compensator, linearly polarized incident beam)

LF in Gauss Laser Beams

(Optical Vortex)

(compensator, laser, circularly polarized incident beam)

Four Stocks parameters universally defying the polarization state of the paraxial Gauss light beam after passing substrate/thin-film system can be written as

$$S_o = 1, \qquad S_1 = -\sigma \sin\delta \sin 2\varphi, \qquad S_2 = \sigma(\sin\Delta\cos\delta + \cos\Delta\sin\delta\cos 2\varphi),$$

$$S_3 = \sigma(-\cos\Delta\cos\delta + \sin\Delta\sin\delta\cos 2\varphi)$$

, where $\sigma=\pm1$ shows right or left polarization of the incident circular Gauss beam, $\Delta=2\pi H\Delta n/\lambda$ (H- film thickness, Δn - optical anisotropy, λ - wavelength), and φ - athimuth. Phase difference, δ, brought-in by the anisotropic substrate is the determinative parameter that depends upon substrate's optical anisotropy and thickness, radial position of the point in the plane of observation and the distance between the entrance (substrate's front surface) and observation planes. A light figure pattern obtained after passing substrate/thin film-compensator-analyzer system is shown below

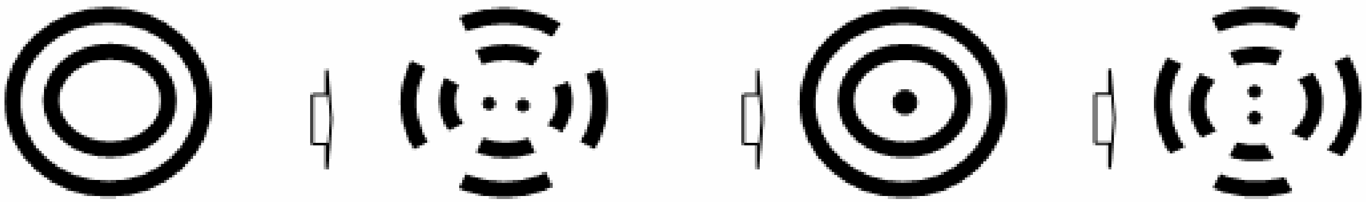

Airy rings **2 OV (l=2)** **1 OV (l=4)**

Studies of the formation of the optical vortexes (OV) with different topological charges (l), and investigation of their spatial patterns is a gate-way to the nanosized thin films.

Conclusions

1. We have suggested **a LF method of the determination of the relative dispersion of the refractive index**, completed numerical and experimental approbation on $CaCO_3$, and shown the overall usefulness of the method for optical characterization of anisotropic materials.
2. We have developed **a first analytical approach to LF of materials with gyration**, received a comprehensive approval for this approach by testing TeO_2, and made a successful experimental demonstration of the predicted **effect of the shrinkage of the interference curves at multiples of π for rotation angle**.
3. Basing on the proposed approximation for radius of an interference curve, **a universal approach to the numbering of the interference curves** has been suggested. The approach has been successfully applied to $CaCO_3$, $AgGaS_2$ and TeO_2.
4. The effectiveness of the LF method for **optical characterization of the modulated structures with correlation length at the nanoscale** has been demonstrated on the novel thallium-contained ternary compounds with incommensurate phase.
5. The **on-going generalization** of the method has been touched briefly by addressing the problems related to both **biaxial material and thin film applications**. **Anisotropic substrates** have been proposed to open **a gateway for application of LF spectroscopy to nanosized thin films**.